Supporting information

Selective Adsorption of CO_2/CH_4, CO_2/N_2 Within a Charged Metal-Organic Frameworks

Lidan Kong,[a] Ruyi Zou,[c] Wenzhu Bi,[c] Ruiqin Zhong,[b] Weijun Mu,[a] Jia Liu,[a] Ray P.S. Han,[a] Ruqiang Zou[a,]*

[a] *College of Engineering, Peking University, Beijing 100871, China. E-mail:ray-han@pku.edu.cn, rzou@pku.edu.cn.*

[b] *State Key Laboratory of Heavy Oil Processing, China University of Petroleum, Beijing, 102249, China*

[c] *College of Chemistry and Molecule Engineering,Zhengzhou Universiy, Zhenzhou 450001, Henan, China*

Synthesis of H_3L

General experiments

All the experiments were conducted under the atmosphere of N_2, unless indicated otherwise. Reagents and drugs were obtained from commercial sources and used without further purification, unless indicated otherwise. Column chromatography was carried out by traditional method with silica-gel 60F (230-400 mesh). ^{1}H-NMR and ^{13}C-NMR spectra were recorded on a Bruker AM-400 spectrometer.

Synthesis of 1-(4-(9H-carbazol-9-yl)phenyl)ethanone.

A mixture of carbazole (1.67 g, 0.01 mol), 1-(4-fluorophenyl)ethanone (1 mL, 0.0083 mol), anhydrous K_2CO_3 (3.5 g), copper (0.3 g) and dry DMSO (20 mL) was heated to 140 °C and stirred for 72 h before being cooled to room temperature. 100 mL water was then added to the reaction solution and the precipitate was collected and dissolved with 100 mL ethyl acetate. The mother solution was evaporated to remove the solvent after being dried over anhydrous Na_2SO_4. The crude product was purified by column chromatography (CH_2Cl_2 /Petroleum Ether = 1:1v/v) and yielded light yellow solid. (1.3 g, 54 %). ^{1}H NMR (400 MHz, $CDCl_3$): δ (ppm) 8.25-8.22(m, 2H, 1 or 8-Carb*H*), 8.18(d, 2H, 3 or 5-Ph-*H*), 7.75-7.72(m, 2H, 4 or 5-CarbH), 7.52(d, 2H, 2 or 6-Ph-*H*), 7.48-7.44(m, 2H,2 or 7-Carb*H*), 7.38-7.34(m, 2H, 3 or 6-Carb*H*).

Synthesis of 1,1'-(9-(4-acetylphenyl)-9H-carbazole-3,6-diyl)diethanone

A solution of 1-(4-(9H-carbazol-9-yl)phenyl)ethanone (0.57 g, 1.89mmol) in CH_2Cl_2 (50 mL) was gradually added to a solution of $AlCl_3$ (1.335g, 10 mmol) in acetyl chloride (7.25 mL) with ice/water bath. The color of the solution turned deep green very fast. The mixture, which turned into deep green quickly, was stirred for 2 hours at room temperature before being poured into large amount of ice VERY SLOWLY. The mixture was stirred overnight and light yellow slurry form was obtained. The organic phase was separated via syringe and the water phase was washed with CH_2Cl_2(3 × 20 mL). The combined organic phases were washed twice with 5% NaOH aqueous solution, dried with anhydrous $MgSO_4$, filtrated and evaporated. Light yellow solid was obtained. (0.70 g, 95 %) ^{1}H NMR (400 MHz, $CDCl_3$): δ (ppm) 8.87(d, 2H, 4 or 5-Carb*H*)(Carb = Carbazole), 8.28(d, 2H, 3 or 5-Ph*H*), 8.17-8.14(dd, 2H, 2 or 7-Carb*H*), 7.72(d, 2H, 2 or 6-Ph*H*), 7.48(d, 2H, 1 or 8-Carb*H*), 2.78(s, 6H, $CarbCOCH_3$), 2.75(s, 3H, $PhCOCH_3$).^{13}C NMR (100 MHz,$CDCl_3$): δ(ppm) 197.3, 196.7, 143.8, 140.5, 136.8, 131.1, 130.4, 127.5, 126.8, 123.7, 122.0, 110.0, 26.8.

Synthesis of 9-(4-Carboxy-phenyl)-9H-carbazole-3,6-dicarboxylic acid (H_3L)

Liquid bromine (0.8 mL) was slowly added to a pre-cooled NaOH aqueous solution (4 M, 11 mL) with stirring until a deep yellow solution was yielded. The fresh NaOBr solution was added to the suspension of 1,1'-(9-(4-acetylphenyl)-9H-carbazole-3,6-diyl)diethanone (0.43 g) in p-dioxane and stirred at 60 °C for 4 hours before being cooled to room temperature. After being quenched by Na_2SO_3 aqueous solution (5%), the reaction mixture was acidified with conc. HNO_3 ($pH < 1$) and filtrated. The precipitate was collected, washed twice with CH_3OH and dried in Infrared oven. Pale white product was obtained. (0.4 g, 85 %). ^{1}H NMR (400 MHz, $CDCl_3$): δ (ppm) 12.89(s, 3H, COO*H*), 8.98(s, 2H, 4 or 5-Carb*H*), 8.26(d, 2H, 3 or 5-Ph*H*), 8.11-8.09(dd, 2H, 2 or 7-Carb*H),* 7.85-7.83(d, 2H, 2 or 6-Ph*H*), 7.53(d, 2H, 1 or 8-Carb*H*). ^{13}C NMR (100 MHz,$CDCl_3$): δ(ppm) 168.0, 143.5, 140.1, 131.9, 130.9, 128.8, 127.3, 124.2, 123.5, 123.2, 110.5.

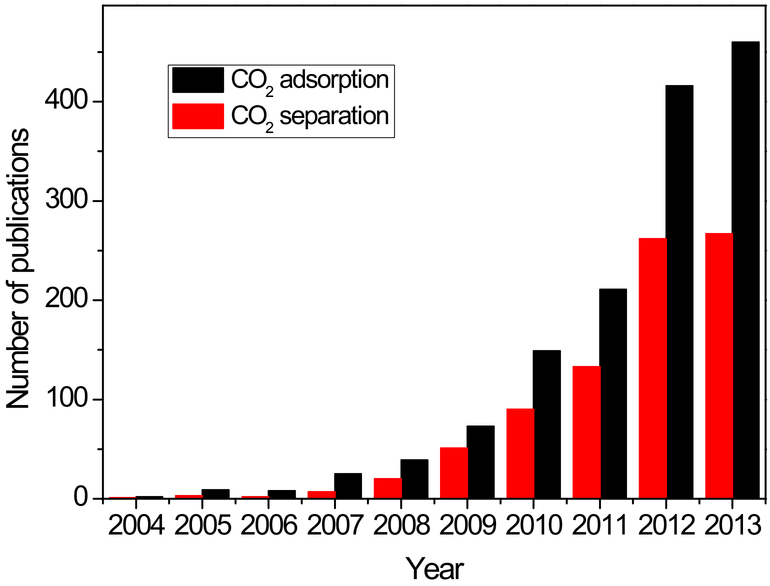

Graph S1. ISI statistical result about CO_2 adsorption and separation.

Table S1. Crystallographic Data and Structural Refinement Summary for **1.**

Formula	$C_{48}H_{37}N_4O_{15.5}Zn_3$
Molecular weight(g/mol)	1101.33
T (K)	293(2)
Crystal system	monoclinic
space group	*C2/c*
a (Å)	20.2644(6)
b (Å)	19.1216(7)
c (Å)	26.8248(8)
Volume (Å^3)	10196.9(6)
α (deg)	90
β (deg)	101.184(3)
γ (deg)	90
Z	8
ρ (g/m^3)	1.43471
R1, wR2 [I>2σ(I)]	0.0786, 0.2165

$R_1=\sum||F_o|-|F_c||/|F_o|$. $wR_2=[\sum w(F_o^2-F_c^2)^2/\sum w(F_o^2)^2]^{1/2}$.

Table S2. Selected bond lengths (Å) and angles (°) of compound **1**.

Zn(1)-O(15)	1.992(6)	O(2)-Zn(1)#2	2.042(5)
Zn(1)-O(1)	2.022(6)	O(3)-Zn(3)#7	1.993(6)
Zn(1)-O(9)#1	2.030(6)	O(3)-Zn(2)#7	2.344(6)
Zn(1)-O(2)#2	2.042(5)	O(4)-Zn(2)#7	2.065(6)
Zn(1)-O(10)#3	2.090(6)	O(5)-Zn(2)#5	2.161(9)
Zn(1)-Zn(1)#2	2.9624(17)	O(6)-Zn(3)#5	1.976(8)
Zn(2)-O(7)	1.968(6)	O(9)-Zn(1)#11	2.030(6)
Zn(2)-O(14)	2.041(6)	O(10)-Zn(1)#3	2.090(6)
Zn(2)-O(13)	2.045(6)	O(11)-Zn(3)#8	1.966(13)
Zn(2)-O(4)#4	2.065(6)	O(13)-Zn(2)#8	2.045(7)
Zn(2)-O(5)#5	2.161(9)	Zn(3)-O(3)#4	1.993(6)
Zn(2)-O(3)#4	2.344(6)	Zn(3)-O(11)#6	1.966(13)
Zn(3)-O(6)#5	1.976(8)	Zn(3)-O(8)	1.968(6)
O(15)-Zn(1)-O(1)	100.3(2)	O(7)-Zn(2)-O(14)	104.3(2)
O(15)-Zn(1)-O(9)#1	100.8(2)	O(7)-Zn(2)-O(13)	88.8(2)
O(1)-Zn(1)-O(9)#1	89.9(2)	O(14)-Zn(2)-O(13)	93.0(2)
O(15)-Zn(1)-O(2)#2	99.9(2)	O(7)-Zn(2)-O(4)#4	151.02(19)
O(1)-Zn(1)-O(2)#2	159.1(3)	O(14)-Zn(2)-O(4)#4	104.39(19)
O(9)#1-Zn(1)-O(2)#2	91.2(2)	O(13)-Zn(2)-O(4)#4	94.0(2)
O(15)-Zn(1)-O(10)#3	99.3(2)	O(7)-Zn(2)-O(5)#5	89.8(3)
O(1)-Zn(1)-O(10)#3	85.9(3)	O(14)-Zn(2)-O(5)#5	82.9(3)
O(9)#1-Zn(1)-O(10)#3	159.3(3)	O(13)-Zn(2)-O(5)#5	175.2(3)
O(2)#2-Zn(1)-O(10)#3	85.9(2)	O(4)#4-Zn(2)-O(5)#5	89.4(2)
O(6)#5-Zn(3)-O(8)	96.0(3)	O(7)-Zn(2)-O(3)#4	91.72(17)
O(6)#5-Zn(3)-O(3)#4	123.4(3)	O(14)-Zn(2)-O(3)#4	162.01(18)
O(8)-Zn(3)-O(3)#4	102.08(19)	O(13)-Zn(2)-O(3)#4	95.6(2)
O(5)#5-Zn(2)-O(3)#4	89.0(2)	O(4)#4-Zn(2)-O(3)#4	59.30(16)

Symmetry transformations used to generate equivalent atoms: #1 x-1/2,y+1/2,z; #2 -x+1,-y+1,-z; #3 -x+3/2,-y+1/2,-z; #4 -x+3/2,y-1/2,-z+1/2; #5 -x+3/2,-y+3/2,-z; #6 x+1/2,-y+1/2,z+1/2; #7 -x+3/2,y+1/2,-z+1/2; #8 x-1/2,-y+1/2,z-1/2; #9 -x+1,y,-z+1/2; #10 -x+1,y,-z+3/2; #11 x+1/2,y-1/2,z.

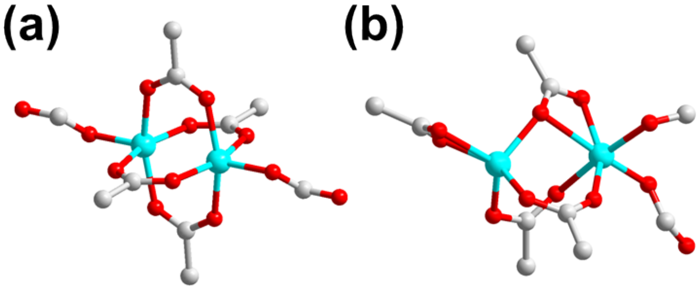

Figure S1. Coordination environment of: (a) symmetric metal cluster; (b) asymmetric metal cluster. Distances between the two Zn atoms are calculated to be 2.961(2) Å and 3.243(2) Å respectively. Zn: light blue; C: grey; O: red.

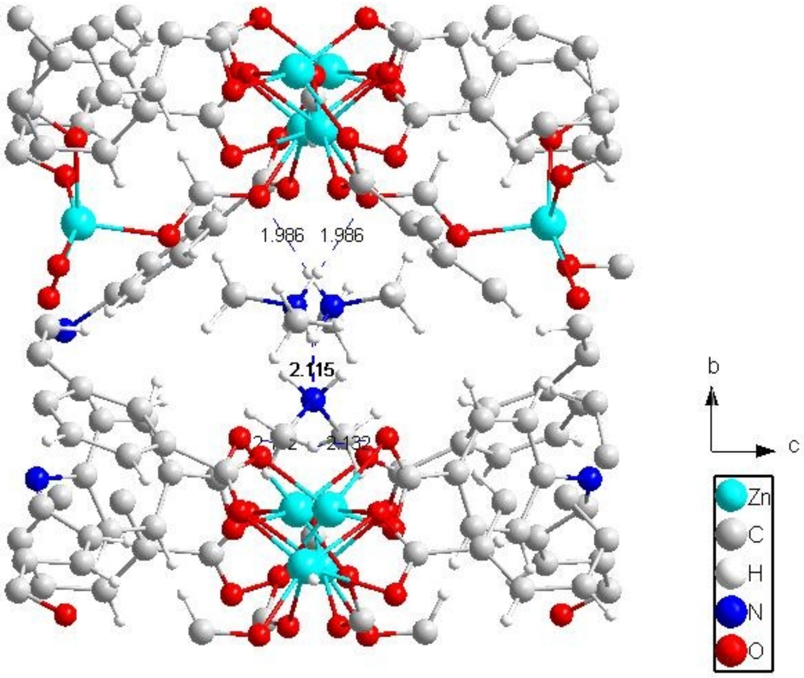

Figure S2. Interaction between DMA$^+$ and the host framework. Hydrogen bond information: bond angle: N(4)-H(4A)···O(14) = 173^o, N(3)-H(4B)···N(4) = 151^o, C(45)-H(45A)···O(12) = 161^o; bond length: H(4A)···O(14) =1.986 Å, H(4B)···N(4) =2.115 Å, H(45A)···O(12) =2.132 Å.

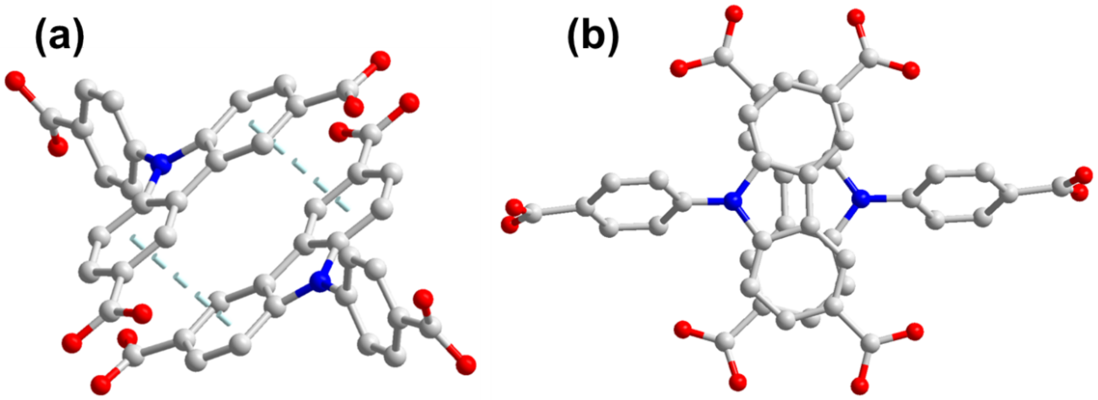

Figure S3. The π-π packing mode of binuclear ligand SUBs with a torsional angle of 64.3(4). $D_{\pi\text{-}\pi}$=3.243(2) Å.

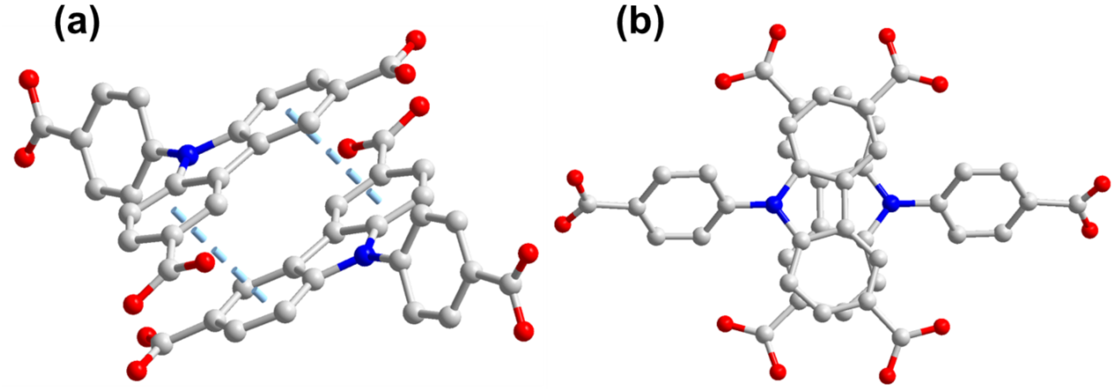

Figure S4. The π-π packing mode of ligand SBUs with a torsional angle of 54.6(4). $D_{\pi\text{-}\pi}$=3.573(2)Å.

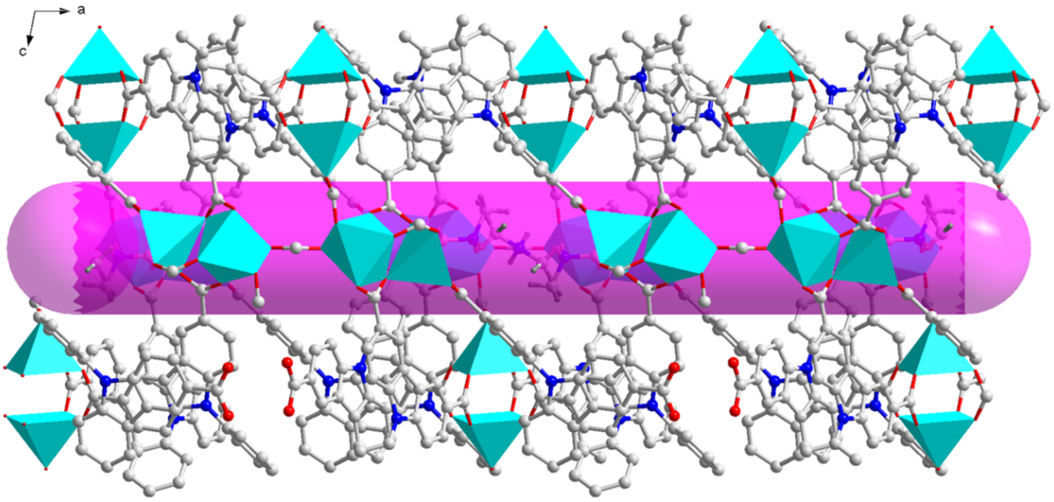

Figure S5. View of the large channel (pink) along ***a*** direction.

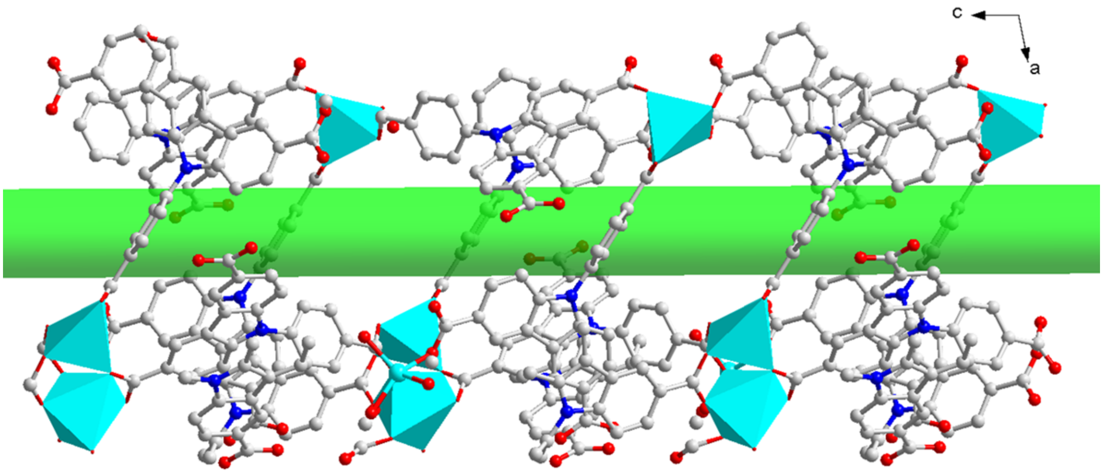

Figure S6. View of the small channel (green) along ***c***direction.

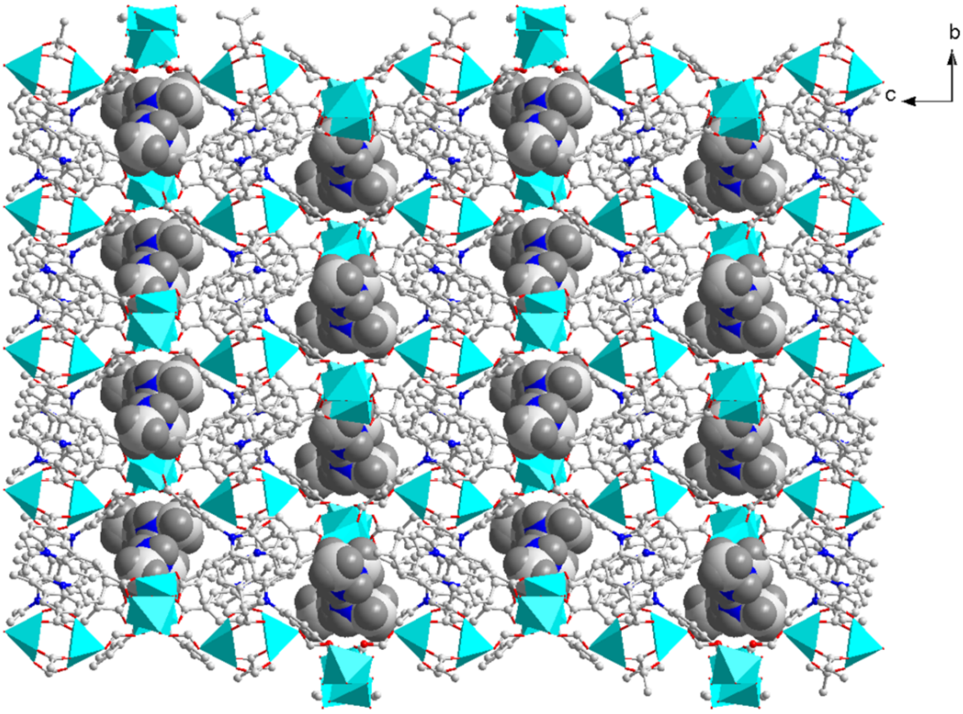

Figure S7. Full view of the large channel along ***a*** direction blocked with DMA^+.

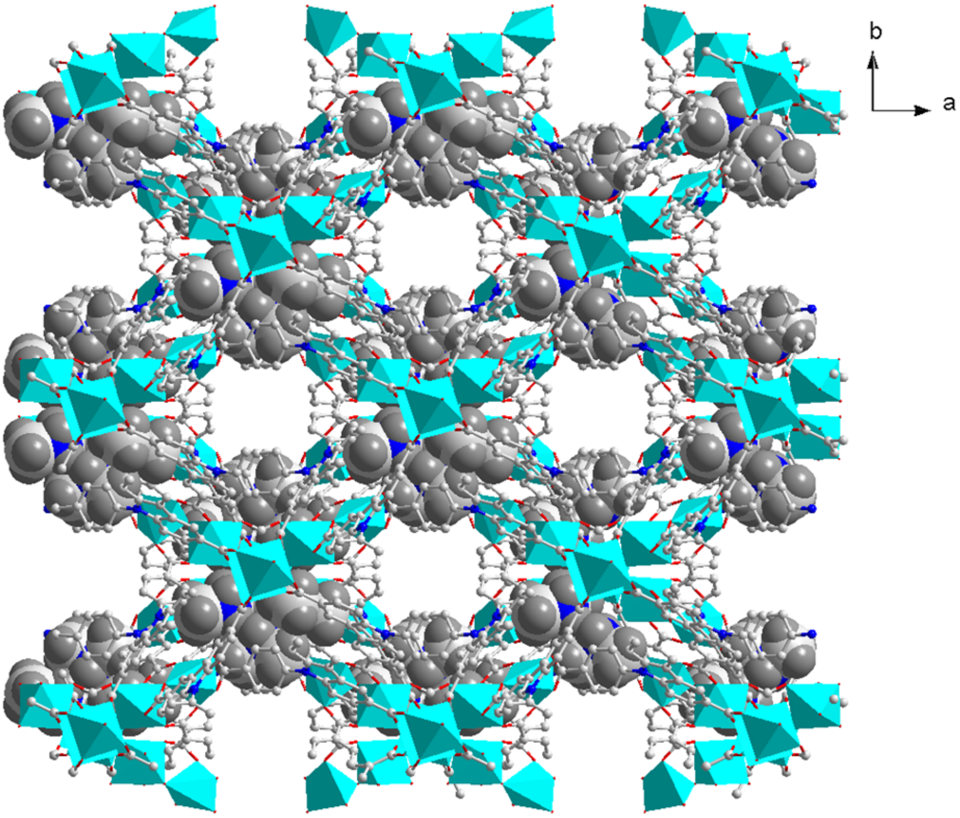

Figure S8. Full view of the small void channel along ***c*** direction .

Table S3. Elemental analysis result for the activated sample before and after cations exchange.

Elemental analysis	C/%	H/%	N/%
Before exchange	49.05	3.45	4.29
After exchange	49.05	3.26	4.30
Theoretical value	49.40	3.50	4.34

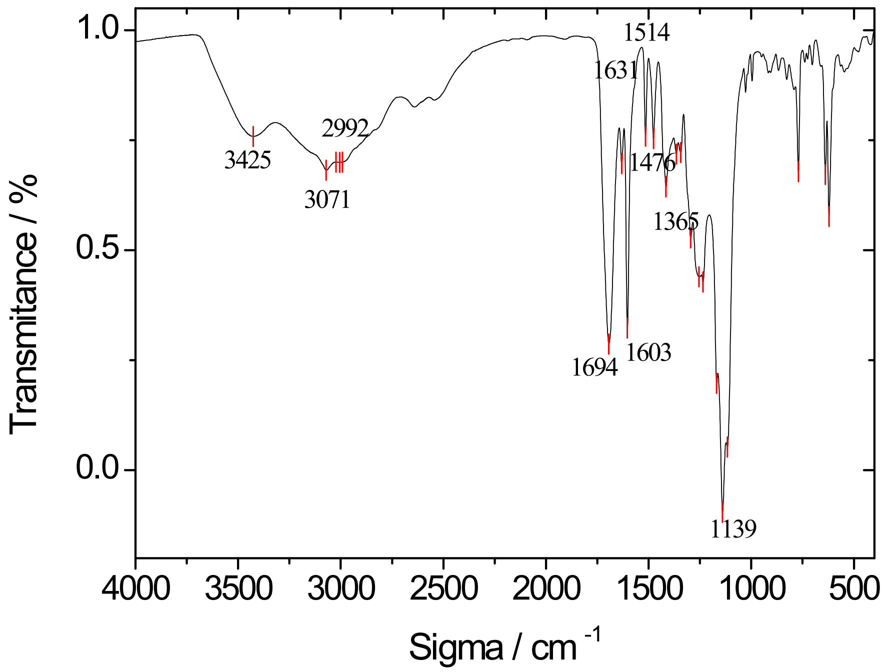

Figure S9. FT-IR spectra for ligand H_3**L** (KBr pellet): 3425(O-H), 3071(C-H), 1694, 1631(O=C-O), 1365(C-N), 1139(C-O).

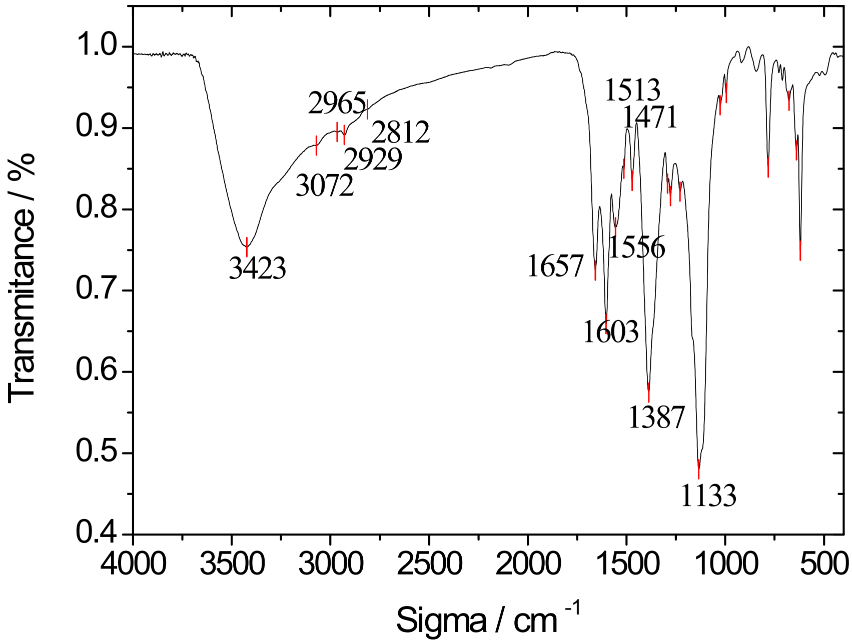

Figure S10. FTIR spectra for **1a** (KBr pellet): 3423(O-H, N-H$_{(DMA+)}$), 3072, 2905, 2929(C-H$_{(Ligand)}$), 1657 (O=C-O), 1471(C-N$_{(DMA+)}$), 1387(C-N$_{(Ligand)}$), 1133(C-O$_{(Ligand)}$).

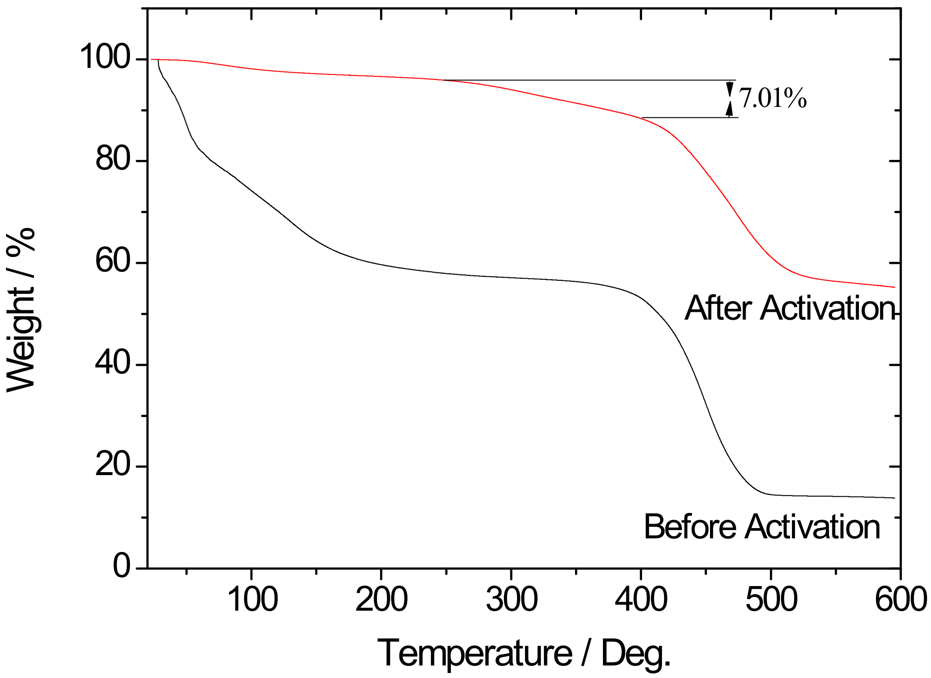

Figure S11. TG curves of **1** and **1a**.

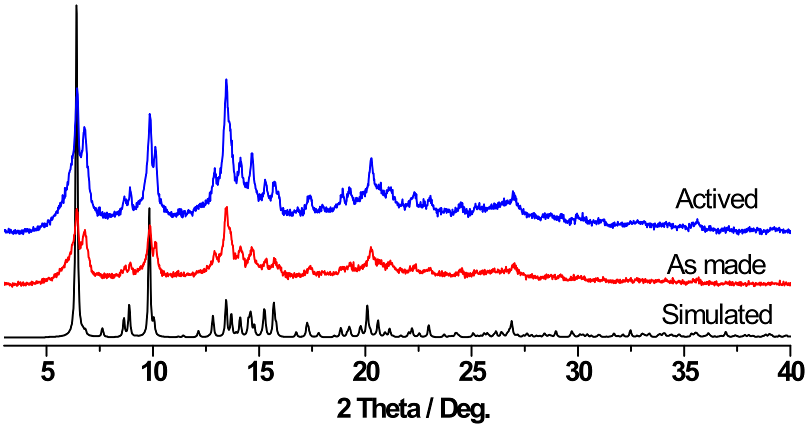

Figure S12. Powder XRD patterns of **1**and **1a**.

Selectivity calculation by Henry' Law based on Langmuir isotherm model:

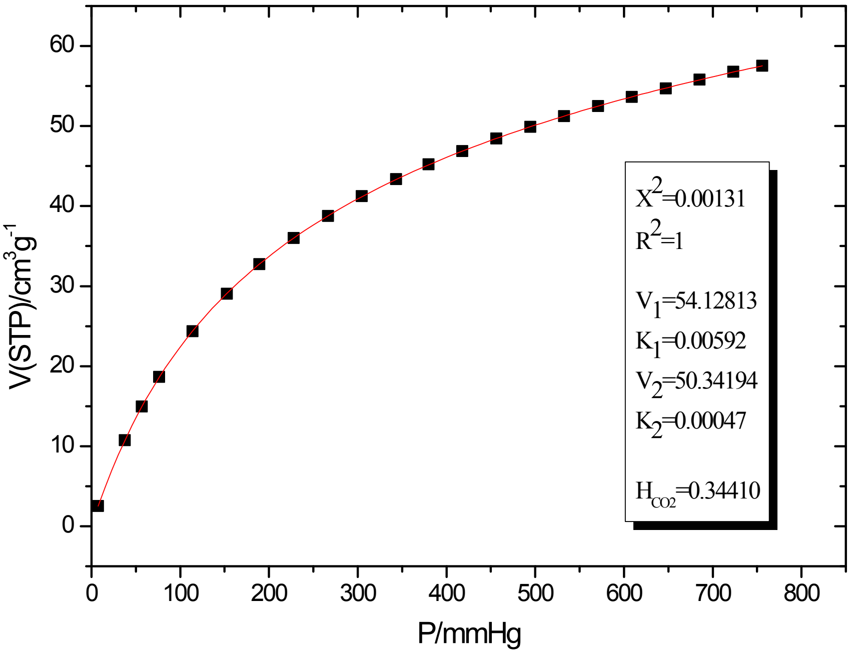

Figure S13. CO_2 isotherm adsorption branch of **1** (filled shape) and fitting based on dual-site Langmuir isotherm model (red line). X^2 and R^2, fitting error; *H*, global Herry's law constant, $H(CO_2)=K_1\times V_1 + K_2\times V_2$ ($cm^3\ g^{-1}\ mmHg^{-1}$).

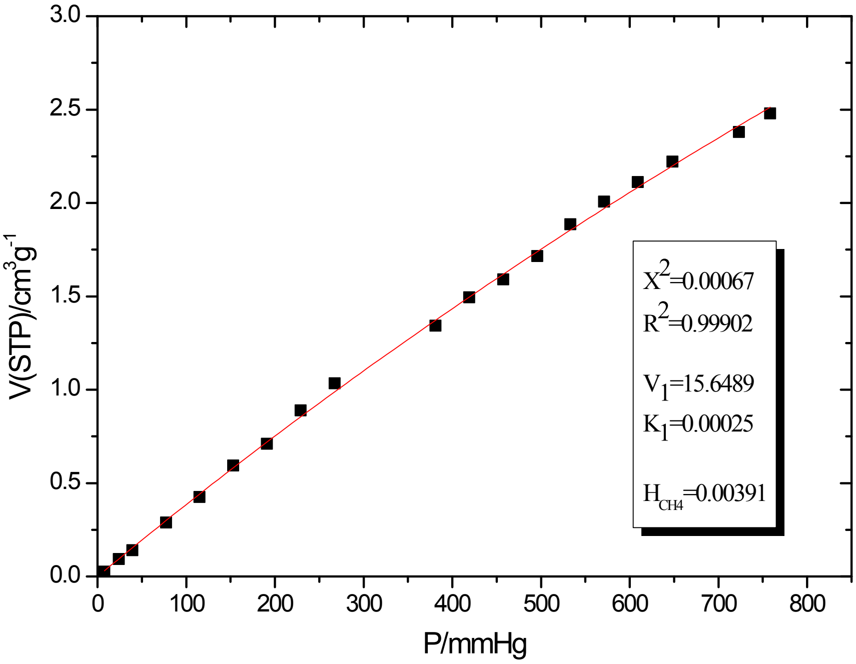

Figure S14. CH_4 isotherm adsorption branch of **1** (filled shape) and fitting based on single Langmuir isotherm model (red line). *V*, calculated adsorbed volume of CH_4; *K*, calculated affinity constants; X^2 and R^2, fitting error; *H*, Herry's law constant, $H(CH_4)=K\times V$ ($cm^3\ g^{-1}mmHg^{-1}$).

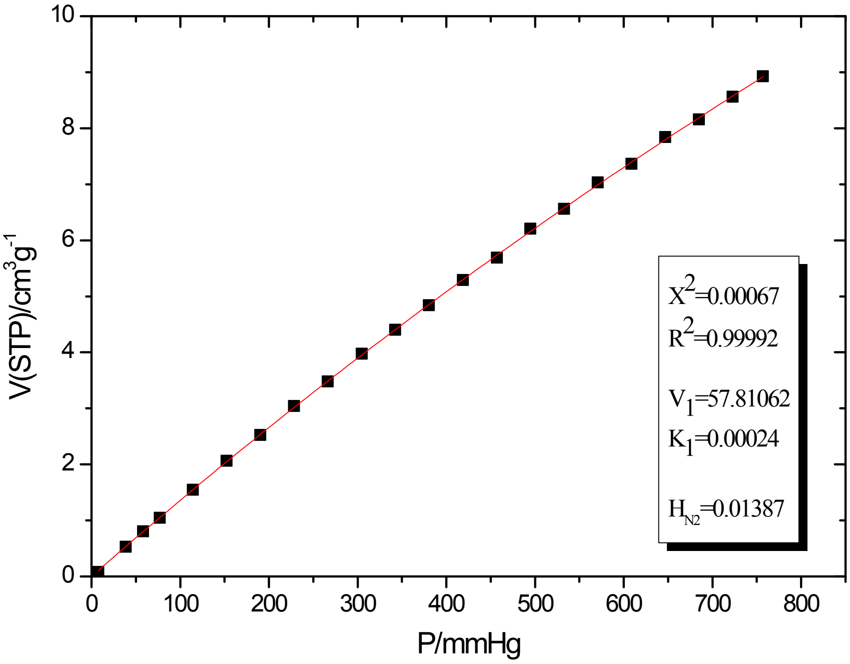

Figure S15. N_2 isotherm adsorption branch of **1** (filled shape) and fitting based on single Langmuir isotherm model (red line). *V*, calculated adsorbed volume of CH_4; *K*, calculated affinity constants; X^2 and R^2, fitting error; *H*, Herry's law constant, $H(N_2)=K\times V$ ($cm^3\ g^{-1}mmHg^{-1}$).

Selectivity calculation by Henry' Law based on Langmuir isotherm model:

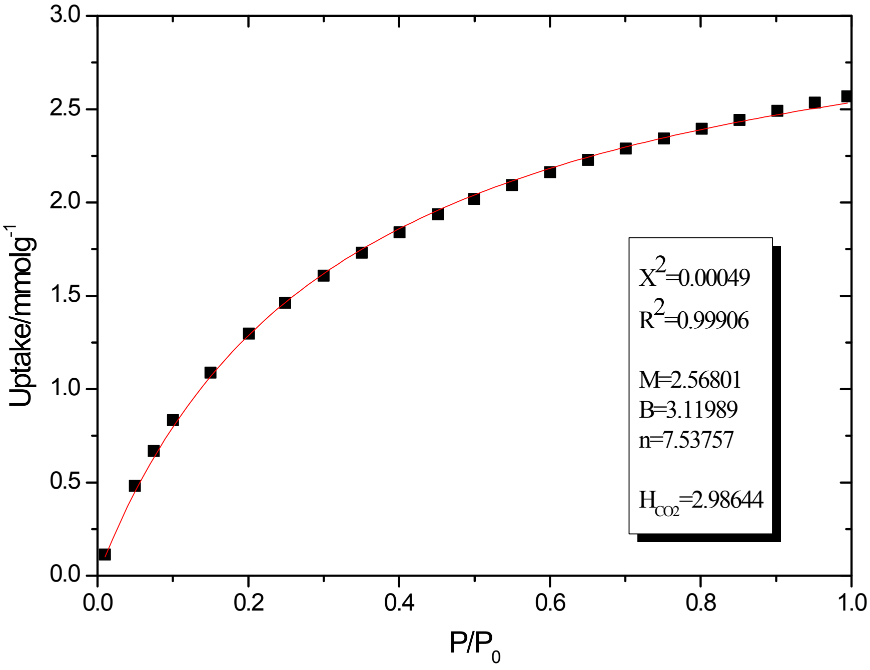

Figure S16. CO$_2$ isotherm adsorption branch of 1 (filled shape) and fitting based on Toth isotherm model (red line); M$_{max}$, maximum uptake amount; B and n, fitting constants; X^2 and R^2, fitting error; H, Henry's law constant.

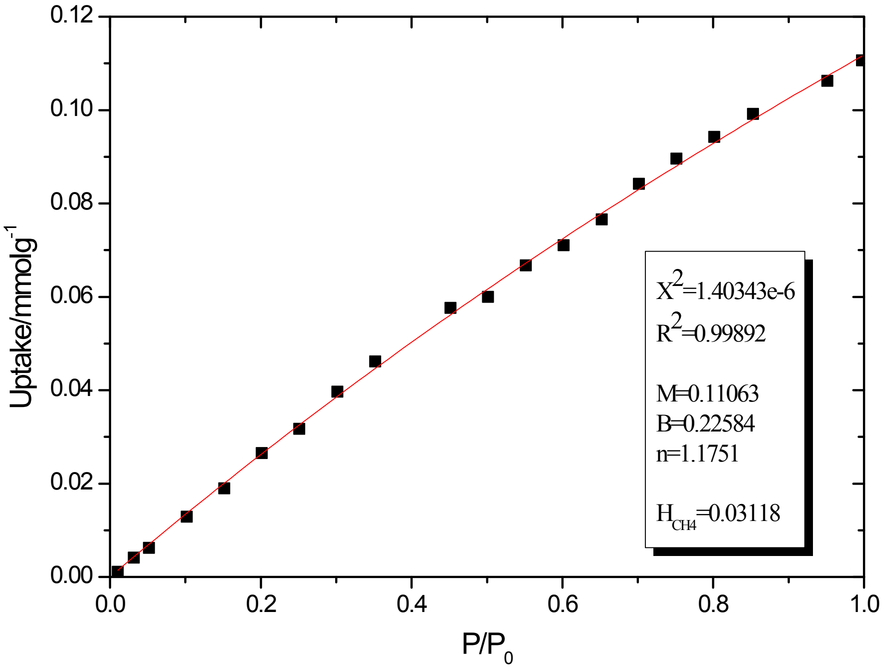

Figure S17. CH_4 isotherm adsorption branch of **1** (filled shape) and fitting based on Toth isotherm model (red line); M_{max}, maximum uptake amount; B and n, fitting constants; X^2 and R^2, fitting error; H, Henry's law constant.

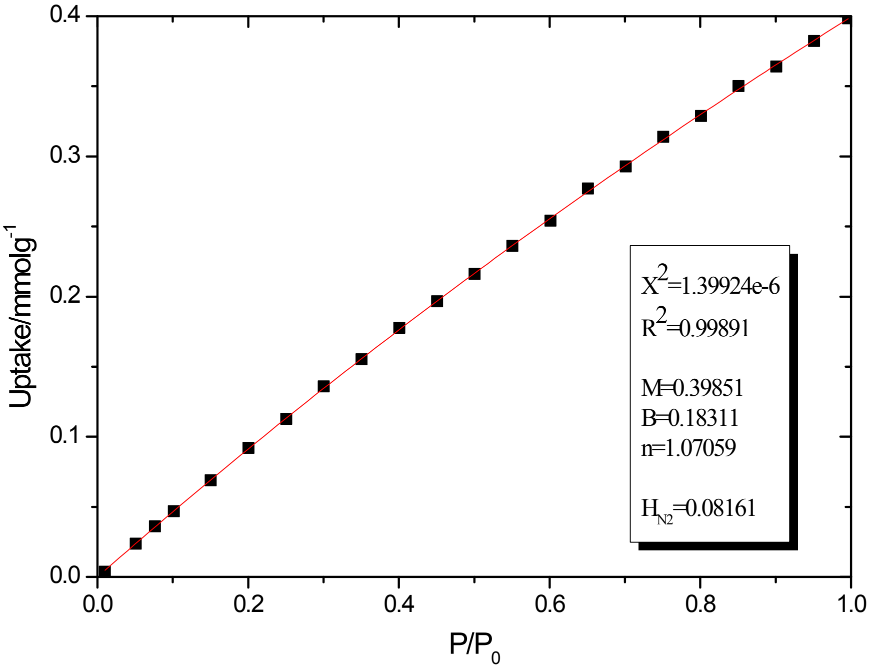

Figure S18. N_2 isotherm adsorption branch of **1** (filled shape) and fitting based on Toth isotherm model (red line); M_{max}, maximum uptake amount; B and n, fitting constants; X^2 and R^2, fitting error; H, Henry’s law constant.

Ideal adsorbed solution theory(IAST)[1].

For the ideal adsorbed solution system, an ideal gas law is obeyed at low surface coverage:

$$\pi_{\left(P_i^0\right)} A = n_i RT \tag{1}$$

$\pi_{\left(P_i^0\right)}$ is spreading pressure of pure component *i*; A, specific surface area of adsorbent; n_i, number of moles of component *i* in adsorbed phase per unit mass of adsorbent; R, ideal gas constant; T, absolute temperature. And:

$$n_i = \int_0^{P_i^0} \frac{n_{i(P)}}{P} dP \tag{2}$$

P_i^0 is the equilibrium pressure for pure component *i* corresponding to spreading pressure $\pi_{\left(P_i^0\right)}$. $n_{i(P)}$, the molar number of the adsorbed gas at given pressure. Here dual-site Langmuir model were used to analyze CO_2 (gas 1) adsorption isotherm, giving the relationship between adsorption amount and relative pressure P.

$$n_{1(P)} = \frac{V_1 K_1 P}{1 + K_1 P} + \frac{V_2 K_2 P}{1 + K_2 P} \tag{3}$$

Similarly, single-site Langmuir model was used to analyze CH_4 and N_2 (gas 2)adsorption isotherms.

$$n_{2(P)} = \frac{V_3 K_3 P}{1 + K_3 P} \tag{4}$$

Here, V_1, V_2 and V_3 are calculated adsorbed volume of the adsorbent; K_1, K_2 and K_3 are calculated stability constants. In the case of binary mixture, the developed pressure of one kind of gas is constantly equivalent to that of the other during the mixing process:

$$\pi_{\left(P_1^0\right)} = \pi_{\left(P_2^0\right)} \tag{5}$$

For given T and A, the combination of equations (1)-(5) yields:

$$\int_0^{P_1^0} \left(\frac{V_1 K_1}{1+K_1 P} + \frac{V_2 K_2}{1+K_2 P}\right) dP = \int_0^{P_2^0} \frac{V_3 K_3}{1+K_3 P} dP \tag{6}$$

By the calculation of integral, relationship between P_1^0 and $P_2^0$is well-determined. In addition, selectivity coefficient ^{2}is defined as:

$$S = \frac{x_1 / y_1}{x_2 / y_2} \tag{7}$$

x_1/x_2, percentage of gas1/gas2 in adsorbed phase; y_1/y_2, percentage of gas1/gas2 in gas phase. And there are:

(8)

(9)

According to Raoult law:

(10)

$$Py_2 = P_2^0 x_2 \tag{11}$$

Here P is the total pressure of gas phase. Since the relationship between P_1^0 and $P_2^0$is well-determined, the value of selectivity is easy to work out according to equations (6)-(11).

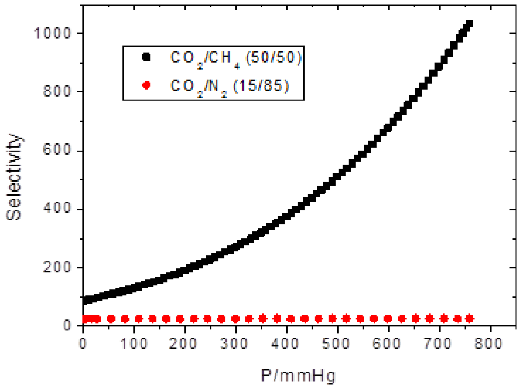

Figure S19. The pressure-dependent selectivity profiles on **1a** **c**alculated by IAST method (273K).

1. A. L. Myers and J. M. Prausnitz, *AIChE. J*, 1965, **11**, 121-127.
2. B. P. Bering and V. V. Serpenskii, *Zhur. Fiz. Khim.*, 1952, **26**, 253-269.